Application of Thermal Effusivity as a Process Analytical Technology Tool for Monitoring and Control of the Roller Compaction Process

Submitted: April 17, 2006; Accepted: August 3, 2006; Published: March 23, 2007

Mohamed K. Ghorab,[1] Ramarao Chatlapalli,[1] Shamim Hasan,[1] and Arwinder Nagi[1]

[1]Solids-Pharmaceutical R&D, Chemical and Pharmaceutical Development, Wyeth Research, Pearl River, NY

ABSTRACT

The aim of this study was to examine the relationship between physical characteristics of compacted ribbons and their thermal effusivity in an attempt to evaluate the feasibility of using effusivity for in-process monitoring of roller compaction. In this study, thermal effusivity, solid fraction, tensile strength, and Young's modulus of ribbons of microcrystalline cellulose (MCC), anhydrous lactose, and placebo (PBO) formulations containing various ratios of MCC to anhydrous lactose (75:20, 55:40, 40:55, and 20:75) were determined at various compaction pressures (25-150 bars). The effusivity–square root of solid fraction relationship was linear for MCC and all the PBO formulations but was a second-order polynomial function for lactose. This could be due to the predominant deformation of lactose by brittle fracture, which might have significantly increased the number and size of contact points between particles, causing a change in thermal conductivity along with a density change. The effusivity–tensile strength and effusivity–Young's modulus relationships were best described by logarithmic functions for MCC but were linear for lactose up to a compaction pressure of 65 bars. There were similar relationships for effusivity with tensile strength and Young's modulus for all PBO formulations except PBO IV, which might have been due to the deformation of lactose, the largest component in this formulation. Strong correlations between effusivity and physical properties of ribbons were established. Although these correlations were formulation-dependent, they demonstrate the possibility of using effusivity as a tool in monitoring roller compaction.

KEYWORDS: Thermal effusivity, roller compaction, solid fraction, tensile strength, Young's modulus.

INTRODUCTION

Over the past few years, there has been increasing interest in implementing innovative technologies for in-process control of unit operations and quality, using design based on good science and an understanding of the operations involved in manufacturing pharmaceutical dosage forms. As a result, process analytical technology has been the focus of the pharmaceutical arena, with many articles,[1-3] meetings, and conferences discussing this subject. This has been complemented by the release of the US Food and Drug Administration guidelines.[4]

Roller compaction is a dry granulation process that involves application of mechanical pressure to powders passing between 2 counterrotating rollers to form compacts,[5,6] which are then milled to form granules of a desirable particle size. The benefit of such a process is powder densification, and improvement of powder flow and content uniformity without the use of solvents. Compaction is a continuous process where the compacts' characteristics, which affect the physical properties of the final granulation, depend to a great extent on the compactor processing parameters used, such as the feeder screw speed, the roll speed, and the compaction pressure.[7,8] Therefore, to maintain the desired quality of the compacts throughout the entire process, a constant powder flow and feed of material to the rolls is required, which might be difficult for poor-flowing powders. Moreover, the heat generated in the nip zone from friction of the rolls with the compacted powder could also cause variation in the properties of compacts over time during the long compaction run of a large batch. Thus, retaining constant process parameters throughout the whole operation does not always guarantee the same compact properties. In-process control and monitoring of compact properties would provide useful feedback for proper adjustment of process parameters, which would maintain the desired quality of compacts as well as granules throughout the batch and thus reduce the intra- and interbatch variability.

Several nondestructive techniques have been reported for the monitoring and control of roller compaction.[9,10] Gupta et al[11] studied the use of near-infrared spectroscopy (NIRS) to examine some key compact attributes, such as content uniformity, moisture content, relative density, tensile strength, and Young's modulus. The authors reported strong agreement between NIRS-predicted values and measurements obtained using reference methods. A strong influence of environmental changes on compact attributes was also found, which further emphasizes the need for real-time monitoring and control of compact properties.

Corresponding Author: Mohamed K. Ghorab, Solids-Pharmaceutical R&D, Wyeth Research, 401 N Middletown Road, Pearl River, NY 10965-1299. Tel: (845) 602-3306; Fax: (845) 602-5529; E-mail: ghorabm@wyeth.com

Thermal effusivity is a nondestructive technique that has only recently been recognized for its pharmaceutical applications. Unlike NIRS, thermal effusivity does not require intense data pretreatment and chemometric data analysis for method development. The technique depends on the heat-transfer property, which is present in all states of matter (solids, liquids, and gases) and is a factor of the thermal conductivity (k), heat capacity (c_p), and density (p) of the material.

$$\text{Effusivity} = \sqrt{\text{k } \rho c_p} \quad (1)$$

Therefore, powders would have different effusivity readings depending on their ability to transfer heat through and between their particles. This is also a function of the particle size, shape, density, and moisture of the material. Mathews et al[12] used effusivity to monitor blend uniformity. Variation in the effusivity readings was expressed in terms of relative standard deviation (%RSD),and was observed to decrease with the progress of the blending run. This observation was attributed to the increase in blend homogeneity, which could be used for the determination of blending end point. However, the blend components used had unique effusivity values, which enabled monitoring of the blend through the change in its effusivity reading. Effusivity has also been used to noninvasively monitor the moisture of granulation during fluid-bed drying for the optimization and control of the drying end point.[13] This was possible due to the much higher effusivity of water (1600 $Ws^{1/2}m^{-2}k^{-1}$) compared with solid pharmaceutical powders (150-800 $Ws^{1/2}m^{-2}k^{-1}$), which resulted in a ~3% increase in powder effusivity with only a 1% increase in moisture content.[13] Roy et al studied the use of thermal effusivity for online monitoring of magnesium stearate lubrication.[14] The increase in blend effusivity during lubrication was reported to be due to the effect of magnesium stearate in decreasing blend porosity and increasing its density. Consequently, this could further be used to monitor and control the lubrication process. However, thermal effusivity's application in monitoring roller compaction has not yet been explored. Therefore, the aim of this study was to examine the relationship between the physical characteristics of compacted ribbons and their thermal effusivity in an attempt to evaluate the feasibility of using effusivity for in-process monitoring of roller compaction.

Materials and Methods

Materials

Avicel PH 101 grade of microcrystalline cellulose (MCC) and croscarmellose sodium were purchased from FMC Corporation (Newark, DE). Anhydrous lactose DT and magnesium stearate were purchased from Quest International (Norwick, NY) and Mallinckrodt (St Louis, MO), respectively.

Preparation of Ribbons

Ribbons of MCC, lactose anhydrous, and placebo formulations (PBO I-IV), the composition of which is shown in Table 1, were prepared using an Alexanderwerk 120 × 40 compactor (Alexanderwerk Inc, Horsham, PA). Roller compaction was done using a screw feeder speed of 40 rpm, a roll speed of 9 rpm, and varying roll pressure of 25, 35, 50, 65, 75, 100, 125, and 150 bars. The surface of the 2 counter-rotating rolls was different: 1 was flat-faced, and the other was knurled. Lubrication of powder MCC or lactose, used in single-component ribbons, with 0.125% magnesium stearate was necessary to prevent ribbons from sticking to the rolls during compaction.

Thermal Effusivity Measurement

Offline thermal effusivity measurements were done on the ribbon's flat face using a BT-08 effusivity sensor (Mathis Instruments Ltd, New Brunswick, Canada). Ribbon samples were cut into 40 × 40 mm segments prior to the measurement and placed on the effusivity sensor in such a way to ensure a complete coverage of the sensor surface by the sample. This was important because there was a slight curvature in the ribbons along the length of the main ribbon sample. Three samples from each batch were measured at each compaction pressure, with replicate readings taken from each sample after 180° sample rotation.

True Density Measurement

The true density of MCC, lactose, and the PBO formulations was determined using an Accupyc 1330 helium pycnometer (Micromeretics Instrument Co, Norcross, GA). All measurements were conducted at 26°C ± 1°C after calibration of the instrument with a standard stainless steel sphere of known mass and volume.

Table 1. Composition of PBO Formulations With Different MCC-to-Lactose Anhydrous Ratios

	Formulation Composition (% wt/wt)			
Ingredients	PBO I	PBO II	PBO III	PBO IV
MCC	75.75	55.75	40	20
Lactose, anhydrous	20	40	55.75	75.75
Croscarmellose sodium	4	4	4	4
Magnesium stearate†	0.125	0.125	0.125	0.125

*PBO indicates placebo; MCC, microcrystalline cellulose.

†This represents only the intragranular portion of lubricant (ie, only 50% of the total magnesium stearate required for the formulation).

Measurement of Solid Fraction

The solid fraction (SF) of the ribbons was determined using the following equation:

$$SF = \frac{\rho_e}{\rho_t} \quad (2)$$

where ρ_e is the envelope density of the ribbon sample and ρ_t is the true density of the material.

The ribbons' envelope density was measured using a Geopyc 1360 envelope density tester (Micromeretics Instrument Co). According to Zinchuk et al,[15] the envelope density could be defined as

$$\rho_e = \frac{m}{V_e} \quad (3)$$

where V_e is the apparent volume of the ribbon samples (including pores and small cavities), and m is the ribbon samples' mass.

Envelope density measurements were conducted in an analyzer chamber 50.8 mm in diameter that was filled with 30 g of DryFlo (Micromeretics Instrument Co., Norcross, GA) (a free-flowing dry medium composed of graphite-lubricated glass microspheres). Six to eight ribbon segments of ~20 mm width were cut from random locations along the length of the ribbons. The ribbon segments were weighed using a Mettler AT261 balance (Mettler-Toledo Inc, Columbus, OH) and placed in the analyzer chamber. Duplicate measurements were conducted on the ribbons from each batch. The number of ribbon segments used per measurement was increased at higher pressures to maintain the percent sample volume at ~25% to 30%. A moderate consolidation pressure of 0.072 MPa was used during measurements to allow for the DryFlo medium to conform to the sample surface without causing changes in the dimensions of the ribbons.

The SF of powder MCC and lactose was calculated using the following equation:

$$SF = \frac{\rho_b}{\rho_t} \quad (4)$$

where ρ_b is the bulk density of the powder sample.

Tensile Strength and Young's Modulus Measurements

The tensile strength (σ_T) and Young's modulus (E) of the ribbons were measured from the load for fracture (F) and the deflection of the midpoint of ribbon segments (ξ) using the 3-point bending method. In this method, the ribbons were cut into 40 mm (length) × 35 mm (width) segments and their F and ξ were measured using a TA.XT.Plus Texture analyzer (Texture Technologies Corp, Scarsdale, NY), with a length (l) of 21 mm between the lower 2 supports. The instrument was calibrated prior to data collection using a 5-kg weight. Measurements were taken at a test speed of 0.1 mm/sec with a trigger force of 0.00981 N and a break sensitivity of 0.09807 N. The tensile strength (σ_T) was calculated from Equation 4:

$$\sigma_T = \frac{3F\,l}{2Wt^2} \quad (5)$$

where W and t are the width and the thickness of the ribbon samples, respectively.

The dimensions of the ribbon samples were measured using a digital caliper. The Young's modulus was derived from the following formula:

$$E = \frac{Fl^3}{4\xi Wt^3} \quad (6)$$

Results and Discussion

MCC and Anhydrous Lactose

In Figure 1, the effusivity of MCC showed a rapid initial increase with compaction pressure up to a pressure of 75 bars, beyond which the rate of effusivity increase slowed down. A similar correlation was observed between the square root of SF and the compaction pressure. Therefore, data describing both the MCC effusivity–compaction pressure and the square root of the SF–compaction pressure relationships were best fitted by a second-order polynomial function ($r^2 = 0.990$ and 0.989, respectively). In contrast to MCC, lactose showed

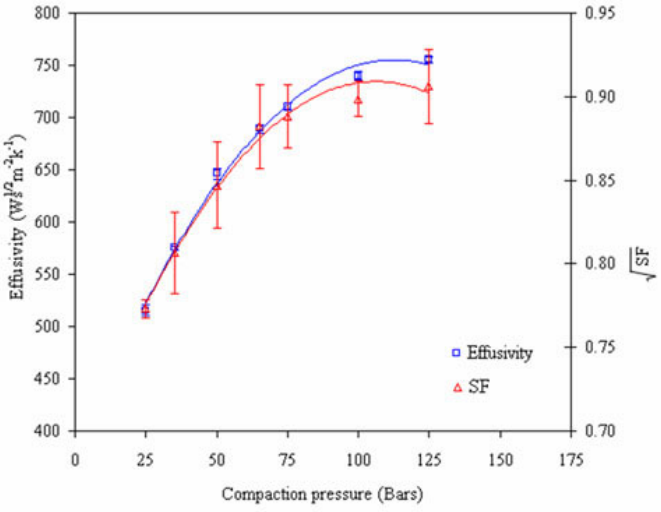

Figure 1. Effect of compaction pressure on effusivity and SF of MCC. SF indicates solid fraction; MCC, microcrystalline cellulose.

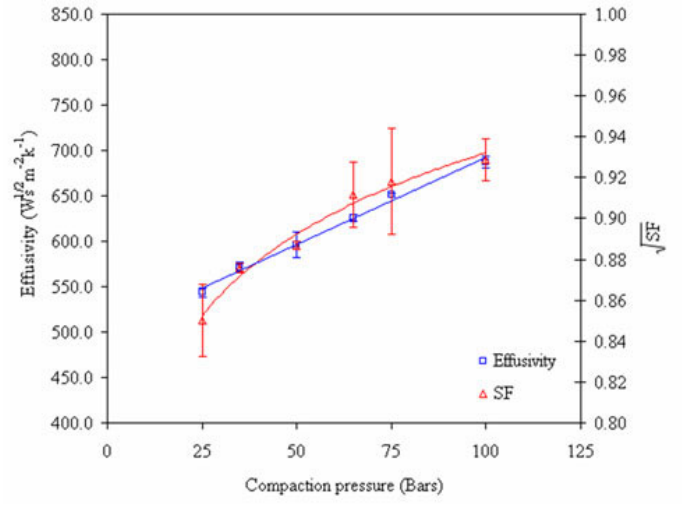

Figure 2. Effect of compaction pressure on effusivity and SF of lactose. SF indicates solid fraction.

a different correlation between effusivity and compaction pressure than between compaction pressure and SF (Figure 2). The rate of increase in lactose effusivity was linear over the compaction pressure range used (r^2 = 0.993), whereas the relationship of the square root of lactose SF with the pressure deviated from linearity and was best described by a second-order polynomial function (r^2 = 0.979). Accurate measurements of effusivity for MCC and lactose ribbons at pressures greater than 125 and 100 bars, respectively, were not achievable because of cracking of ribbon edges and the inability to get intact ribbons at these higher pressures.

Figure 3 illustrates the difference in the effusivity–square root of SF relationship between MCC and lactose, which was in agreement with the above observations. This difference could be attributed to the deformation behavior of these

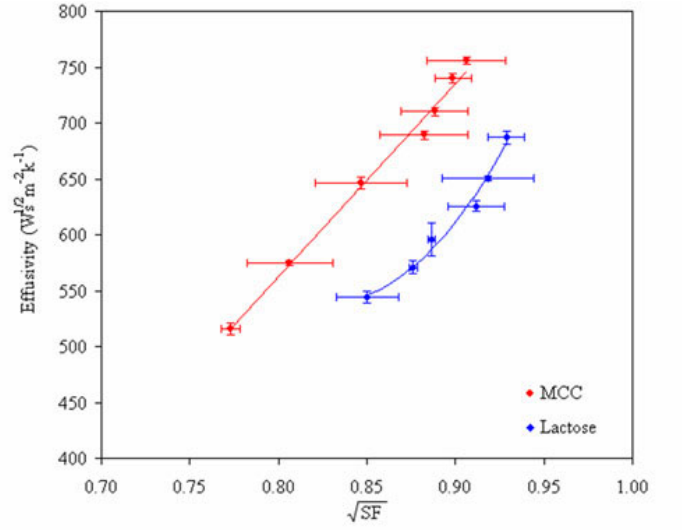

Figure 3. Effusivity–solid fraction profile for MCC and lactose ribbons compacted at various pressures. MCC indicates microcrystalline cellulose.

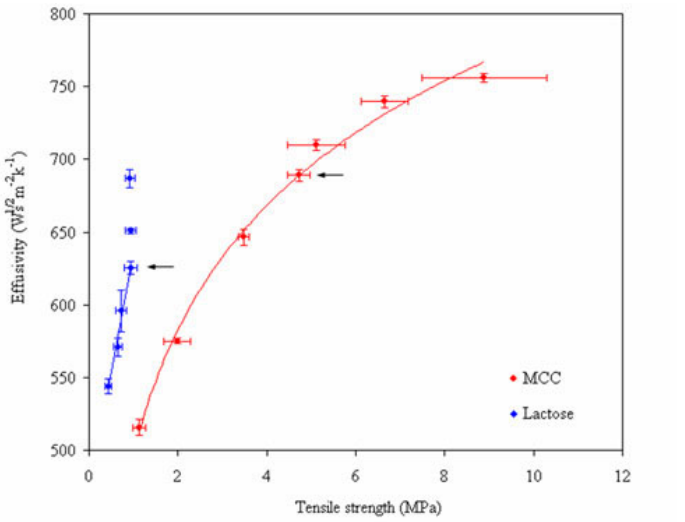

Figure 4. Effusivity vs tensile strength profiles for MCC and lactose ribbons compacted at various pressures. The arrows point to data generated at 65 bars of compaction pressure. MCC indicates microcrystalline cellulose.

2 materials under compression, where lactose predominantly deformed by brittle fracture while MCC underwent plastic deformation. As can be deduced from Equation 1, an increase in SF or density of ribbons of both materials upon compression will increase effusivity. However, the remarkable fragmentation of lactose, with the formation of smaller-sized particles, changed the size of contact points between the particles and consequently influenced the thermal conductivity parameter of effusivity.[16] This increase in contact points was not accompanied with more consolidation and

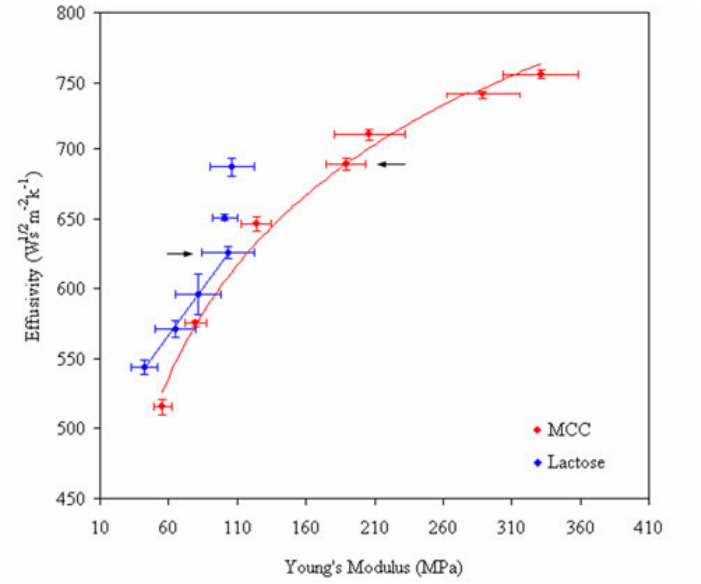

Figure 5. Effusivity vs Young's modulus profiles for MCC and lactose ribbons compacted at various pressures. The arrows point to data generated at 65 bars of compaction pressure. MCC indicates microcrystalline cellulose.

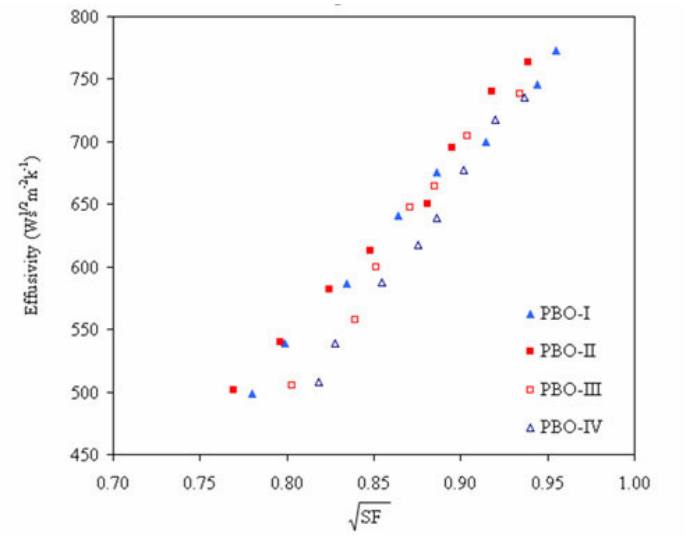

Figure 6. Effusivity–square root of solid fraction relationship for ribbons of PBO formulations. PBO indicates placebo.

an increase in SF at the high compaction pressure, which could have been due to the fact that at the high pressure most of the lactose ductility might have been lost and thus, not enough plastic deformation was available to allow for strong consolidation to occur. Thus, the change in lactose effusivity with compaction pressure was dependent not only on densification and increase in SF but also on the size of the fractured particles and their contact points. However, for MCC, where plastic deformation was more dominant, the change in points of contacts between particles might not have a significant effect on thermal conductivity. Thus, the change in MCC effusivity with an increase in compaction pressure was mainly dependent on the change in SF. As a result, the relationship of effusivity with SF observed in Figure 3 was linear for MCC but not for lactose.

A unique correlation was observed between the ribbons' tensile strength and their effusivity for the 2 materials (Figure 4). MCC displayed a logarithmic profile, whereas lactose was linear up to a tensile strength corresponding to a compaction pressure of 65 bars. Beyond that pressure, no further increase in the tensile strength of lactose ribbons was observed; however, their effusivity was still increasing with pressure. The relatively poor consolidation of lactose beyond a pressure of 65 bars might be the reason for the lack of increase in tensile strength. However, the further increase in effusivity might be attributed to particle fragmentation, which might have still been occurring at pressures higher than 65 bars, increasing the contact points between the particles and the thermal conductivity of the ribbons, as mentioned earlier.

In Figure 5, the effusivity versus Young's modulus profiles for MCC and lactose showed trends similar to those observed between effusivity and tensile strength: MCC's effusivity escalated logarithmically with Young's modulus, but lactose's effusivity increased linearly up to a pressure of 65 bars. These results indicated that effusivity–tensile strength and effusivity–Young's modulus relationships were similar for a particular material, although both were material dependent.

PBO Formulations

MCC and lactose are very frequently used as excipients in formulation development, either alone or in combination, because of the better compaction obtained with a mixture of

Table 2. Best-Fitting Equations Derived From the Relationship of Ribbons' Effusivity With Compaction Pressure and Physical Properties*

	Compaction Pressure	Solid Fraction	Tensile Strength	Young's Modulus
MCC	$y = -0.0299x^2 + 6.7685x + 372.23$ $R^2 = 0.9936$	$y = 1033.2x - 100.25$ $R^2 = 0.9920$	$y = 123.34\text{Ln}(x) + 497.41$ $R^2 = 0.9915$	$y = 93.882\text{Ln}(x) + 224.04$ $R^2 = 0.9923$
Lactose	$y = 1.9061x + 501.07$ $R^2 = 0.9927$	$y = 4205.6x^2 - 5702.1x + 2470.3$ $R^2 = 0.9821$	$y = 160.25x + 474.41$ $R^2 = 0.9733$	$y = 1.3455x + 482.74$ $R^2 = 0.9497$
PBO I	$y = -0.0136x^2 + 4.5229x + 396.86$ $R^2 = 0.9929$	$y = 861.58x - 13.449$ $R^2 = 0.9913$	$y = 106.02\text{Ln}(x) + 541.82$ $R^2 = 0.9898$	$y = 118.46\text{Ln}(x) + 69.96$ $R^2 = 0.9857$
PBO II	$y = -0.0107x^2 + 3.9434x + 411.92$ $R^2 = 0.9994$	$y = 917.9x - 44.29$ $R^2 = 0.9922$	$y = 95.516\text{Ln}(x) + 568.63$ $R^2 = 0.9815$	$y = 113.9\text{Ln}(x) + 104.5$ $R^2 = 0.9788$
PBO III	$y = -0.0165x^2 + 4.6809x + 405.83$ $R^2 = 0.9963$	$y = 1076.6x - 184.78$ $R^2 = 0.9772$	$y = 88.187\text{Ln}(x) + 613.55$ $R^2 = 0.9936$	$y = 93.882\text{Ln}(x) + 224.04$ $R^2 = 0.9923$
PBO IV	$y = -0.0099x^2 + 3.5146x + 429.4$ $R^2 = 0.9979$	$y = 1094.1x - 217.1$ $R^2 = 0.9931$	$y = -21.674x^2 + 152.71x + 471.2$ $R^2 = 0.9971$	$y = 1.4341x + 484.98$ $R^2 = 0.9826$

*MCC indicates microcrystalline cellulose; PBO, placebo. y indicates effusivity; x, physical property.

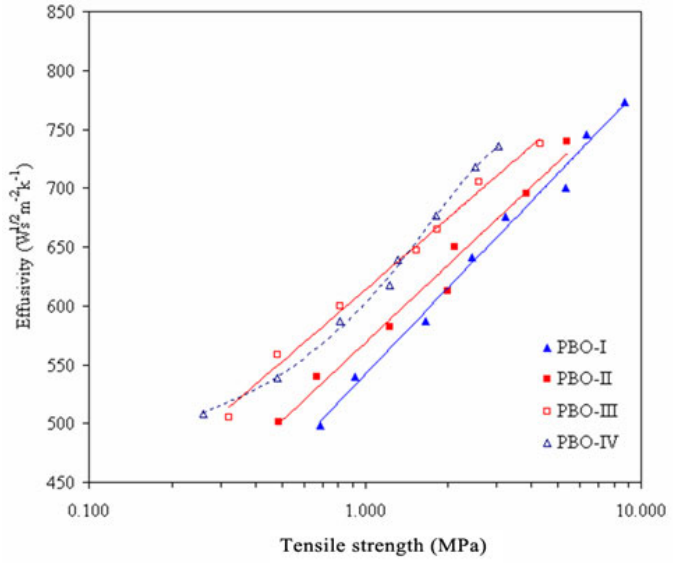

Figure 7. Effusivity–tensile strength relationship and effusivity for ribbons of PBO formulations. PBO indicates placebo.

plastic deformation and brittle fracture of particles. Therefore, in this study the 4 placebo formulations (PBO I to PBO IV) presented in Table 1 were used to examine the effect of varying the MCC-to-lactose ratio on the physical properties and effusivity of the resulting ribbons.

For all 4 PBO formulations, the effusivity–compaction pressure and the square root of SF–compaction pressure profiles were best fitted by second-order polynomial functions (data not shown). Therefore, in Figure 6 the data points describing the relationships between effusivity and square root of SF for these formulations were best described by linear regression models similar to those of MCC (Table 2).

However, the logarithmic profile for the effusivity versus tensile strength behavior, which was observed for the MCC ribbons in Figure 3 and Table 2, was not seen for all the PBO formulations. The PBO IV formulation, which had ~75% lactose, showed deviation in its effusivity–tensile strength profile compared with the other 3 formulations (Figure 7). The fact that the second-order polynomial function model (Table 2) fit the PBO IV formulation better than a logarithmic one did was probably due to change in the main deformation behavior, from plastic deformation to brittle fracture, as lactose became the predominant ingredient in the formulation. A similar change was also observed in the relationship between effusivity and Young's modulus for PBO IV, where the amount of lactose in the formulation was more than 3 times higher than that of MCC (data not shown).

This showed that for formulations composed mainly of MCC and lactose, there were strong correlations between changes occurring in the physical properties of the ribbons and their effusivity as compaction pressure was changed. The type of these correlations tended to vary as the MCC-to-lactose ratio in the formulation changed. However, the effusivity-SF relationship was less sensitive to the change in the MCC-to-lactose ratio compared with the relationship of effusivity with tensile strength or Young's modulus.

Figures 8 and 9 further illustrate the effect of the MCC-to-lactose ratio on the square root of SF and tensile strength. The effect of the MCC-to-lactose ratio on the square root of SF showed a sigmoidal pattern (Figure 8). The SF value showed an initial decrease with the increase in the MCC-to-lactose ratio, because MCC had a lower SF than lactose did. However, this decrease in SF occurred only to a MCC-to-lactose ratio of ~2. After that, the SF increased with the increase in the MCC-to-lactose ratio to the extent that the SF of the highest ratio used in PBO I (3.75) surpassed that of the lowest ratio of PBO IV (0.267). This was more noticeable at the higher compaction pressures and was probably due to

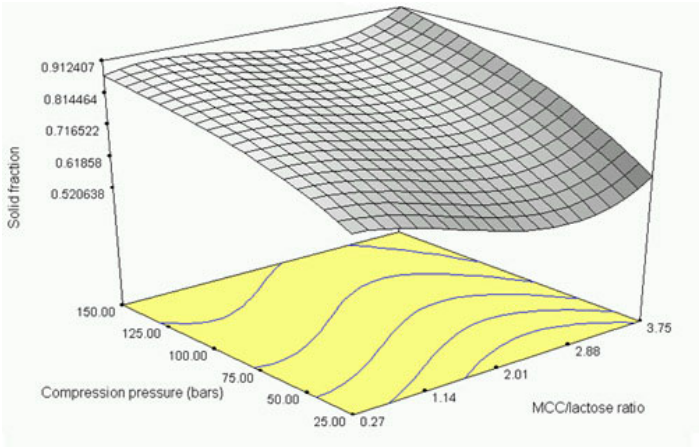

Figure 8. Three-dimensional plot of the effect of compaction pressure and MCC-to-lactose ratio in placebo formulations on the solid fraction of ribbons. MCC indicates microcrystalline cellulose.

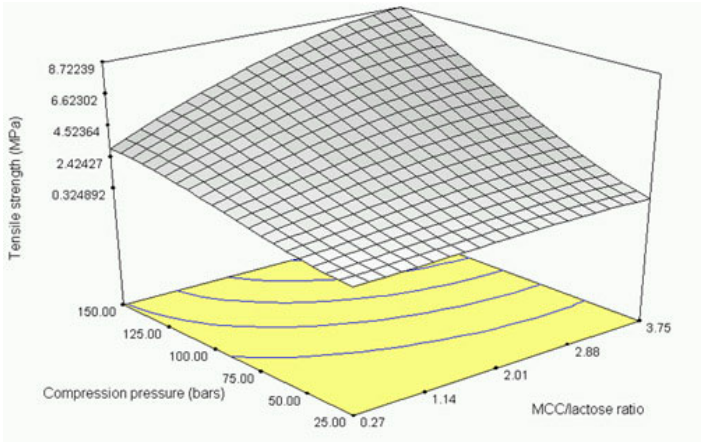

Figure 9. Three-dimensional plot of the effect of compaction pressure and MCC-to-lactose ratio in PBO formulations on the tensile strength of ribbons. MCC indicates microcrystalline cellulose.

the better compressibility of MCC compared with lactose, which caused more densification as the MCC-to-lactose ratio increased with the elevation in compaction pressure. For that same reason, the tensile strength of ribbons showed a significant increase with the rise in the MCC-to-lactose ratio at higher compaction pressures, whereas at low compaction pressures the increase in tensile strength was not remarkable to the same extent (Figure 9).

It is important to mention that reliable and accurate effusivity readings were obtained only when the flat face of short segments of ribbons was entirely covering the sensor. The use of the knurled side of ribbons resulted in erroneous readings because air pockets would get trapped between the knurls and the sensor. Incorrect readings were also obtained with long ribbons, even with the flat side facing the sensor, because their curvature left part of the sensor uncovered.

Effusivity reading requires a few seconds of static direct contact between the sensor and the ribbon in addition to ~30 seconds of sensor cooling time. This might make it difficult for effusivity to be used for online monitoring of roller compaction unless further instrumental improvement reduces the cooling time required between measurements.

CONCLUSION

Effusivity had strong correlations with the physical properties of compacted ribbons, which could be used to monitor these properties. However, there are still some hurdles that need to be addressed before effusivity can be used for online process monitoring of roller compaction. Future studies will be conducted to evaluate the effect of lot-to-lot variability and the impact of the physical characteristics of active ingredients in the formulations on the correlations established between effusivity and the properties of ribbons.

REFERENCES

1. Shenoy P. Process analytical technology. *Pharma Times.* 2004; 36:37–38.

2. Davis TD, Morris KR, Huang HP, et al. In situ monitoring of wet granulation using online x-ray powder diffraction. *Pharm Res.* 2003;20:1851–1857.

3. Balboni ML. Process analytical technology: concepts and principles. *Pharm Technol.* 2003;27:54–66.

4. US Food and Drug Administration. *PAT—A Framework for Innovative Pharmaceutical Development, Manufacturing, and Quality Assurance, Guidance for Industry.* Washington, DC: US Food and Drug Administration, Center for Drug Evaluation and Research; 2004.

5. Miller RW. Roller compaction technology. In: Parikh DM, ed. *Handbook of Pharmaceutical Granulation Technology.* New York, NY: Marcel Dekker; 1997:99–149.

6. Adeyeye MC. Roller compaction and milling pharmaceutical unit processes: part I. *Am Pharm Rev.* 2000;3:37–42.

7. Falzone AM, Peck GE, McCabe GP. Effects of changes in roller compactor parameters on granulations produced by compaction. *Drug Dev Ind Pharm.* 1992;18:469–489.

8. Jerome E, Delacourte A, Leterme P, Guyot JC. The measurement of resulting forces on a roller compactor. *Drug Dev Ind Pharm.* 1991;17:1571–1591.

9. Gupta A, Peck GE, Miller RW, Morris KR. Nondestructive measurements of the compact strength and the particle-size distribution after milling of roller compacted powders by near-infrared spectroscopy. *J Pharm Sci.* 2004;93:1047–1053.

10. Hakanen A, Laine E. Acoustic characterization of a microcrystalline cellulose powder during and after its compression. *Drug Dev Ind Pharm.* 1995;21:1573–1582.

11. Gupta A, Peck GE, Miller RW, Morris KR. Real-time near-infrared monitoring of content uniformity, moisture content, compact density, tensile strength, and Young's modulus of roller compacted powder blends. *J Pharm Sci.* 2005;94:1589–1597.

12. Mathews L, Chandler C, Dipali S, et al. Monitoring blend uniformity with effusivity. *Pharm Technol.* 2002;26:80–84.

13. Roy Y, Closs S, Mathis N, Nieves E. Thermal effusivity as a process analytical technology to optimize, monitor and control fluid-bed drying. *Pharm Technol.* 2004;28:21–28.

14. Roy Y, Mathis N, Closs S, et al. Online thermal effusivity monitoring: a promising technique for determining when to conclude blending of magnesium stearate. *Tablets Capsules.* 2005;3:38–47.

15. Zinchuk AV, Mullarney MP, Hancock BC. Simulation of roller compaction using a laboratory scale compaction simulator. *Int J Pharm.* 2004;269:403–415.

16. Shapiro M, Dudko V, Royzen V, et al. Characterization of powder beds by thermal conductivity: effect of gas pressure on the thermal resistance of particle contact points. *Part Part Syst Char.* 2004;21: 268–275.